Dear Author

Please use this PDF proof to check the layout of your article. If you would like any changes to be made to the layout, you can leave instructions in the online proofing interface. Making your changes directly in the online proofing interface is the quickest, easiest way to correct and submit your proof. Please note that changes made to the article in the online proofing interface will be added to the article before publication, but are not reflected in this PDF proof.

If you would prefer to submit your corrections by annotating the PDF proof, please download and submit an annotatable PDF proof by clicking here and you'll be redirected to our PDF Proofing system.

Measurement xxx (xxxx) xxx

Contents lists available at ScienceDirect

Measurement

journal homepage: www.elsevier.com/locate/measurement

Comparative of conventional and alternative Digital Image Correlation techniques for 3D modal characterisation

Ángel J. Molina-Viedma [a,*], Luis Felipe-Sesé [b], Elías López-Alba [a], Francisco A. Díaz [a]

[a] Departamento de Ingeniería Mecánica y Minera, Campus Las Lagunillas, Universidad de Jaén, 23071 Jaén, Spain
[b] Departamento de Ingeniería Mecánica y Minera, Campus Científico Tecnológico de Linares, Universidad de Jaén, 23700 Linares, Spain

ARTICLE INFO

Article history:
Received 31 May 2019
Received in revised form 4 September 2019
Accepted 23 September 2019
Available online xxxx

Keywords:
3D modal analysis
Single camera
Digital Image Correlation
Fringe Projection

ABSTRACT

The integration of Fringe Projection and 2D-DIC is a low-cost optical technique which employs a single camera for full-field 3D displacement measurements using RGB colour encoding to filter coexisting fringe and speckle patterns out from a single image. In this work, this technique was explored together with conventional 3D-DIC for challenging modal analysis on a large aeronautical panel under random excitation. Modal identification was performed using the Least-Squares Complex Exponential approach. Multiple degree-of-freedom methods have been avoided in previous works or just employed in one direction due to high memory requirements to process 3D full-field data. In this work, the 3D modal characterisation was addressed with especial mention to mode shapes. Hardware limitations makes FP + DIC less sensitive than 3D-DIC and hence more suitable for lower frequencies. Nevertheless, the obtained modal parameters showed high agreement and hence FP + DIC demonstrated to be a cost-effective alternative for 3D modal analyses.

1. Introduction

In the last decades, experimental mechanics have exploited the full-field information provided by Digital Image Correlation (DIC) techniques [1,2]. These techniques originally came up for in-plane displacement measurements using a single camera what nowadays is known as two-dimensional DIC (2D-DIC). Using an analogous correlation procedure and an appropriate calibration, three dimensional DIC (3D-DIC) expanded the use of DIC to more complex 3D shape and deformations thanks to pairs of images from a stereoscopic system. These full-field displacement and also strain 3D measurements gave experimentalists the chance to cover their topics in an unprecedented manner. Despite those benefits, this involves costs increment for equipment due to the additional camera and synchronisation devices. That is especially relevant in dynamics events considering the high cost of high speed cameras. Hence, 3D-DIC is not always affordable and hence single-camera DIC-based techniques have been developed in the search for economic alternatives for 3D measurements. Some of them are based on 3D-DIC and manage to combine two points of view in a shared single image using different optical arrangements composed of diffraction grating, bi-prisms or, especially, mirrors [3,4].

From a different perspective, 3D measurements were achieved by combining two different techniques like 2D-DIC and Fringe Projection [5]. Fringe Projection (FP) is based on the oblique projection of a sinusoidal fringe pattern over the specimen. The out-of-plane displacement (in Z- direction) leads to a lateral shift of that projected pattern over the specimen. This Z measurement is related to variation of phase of the sinusoidal projected fringe pattern. Hence, whereas 2D-DIC offers in-pane displacement measurements (in X and Y directions), FP contributes with the Z measurement. Finally, both sets of information must be combined through a recent methodology [6,7] to extract the actual displacement maps in the X, Y, and Z directions. The combination of both optical techniques relies on the capturing of colour images and RGB colour pattern encoding [8] which allows to separate different fringe and speckle patterns. Then, filtered images are suitable to be independently processed. The experimental set up is reduced to a colour camera and a projector that obliquely projects a fringe pattern. One of the strengths of this integration in comparison to previous single-camera 3D-DIC based approaches is that the field of view is not reduced and hence the set-up is more versatile, especially when large field of view is required. Complex and delicate optic arrangements are neither required in the set-up. However, the definition of patterns depends on the sensitivity of the camera to colours and some noise could reciprocally affect the patterns. Additionally, as inclination and period of projected fringes will

* Corresponding author.
E-mail address: ajmolina@ujaen.es (Á.J. Molina-Viedma).

https://doi.org/10.1016/j.measurement.2019.107101
0263-2241/

define the sensitivity of out-of-plane displacements, different sensitivities could be achieved for in- and out-of-plane displacements [9].

A discipline where DIC have recently achieved high relevance is experimental modal analysis as an alternative to conventional pointwise, invasive transducers [10]. The spatial information for high detailed mode shapes has been an important attraction for many researchers who obtained it from simple forced resonance tests [11–16]. For complete modal analysis, the elevated number of data points implies high computational memory demand [17], what may not be always accomplished. For this reason, most of the studies are devoted to mode shape characterisation using sinusoidal signals or modal identification using single degree-of-freedom (SDOF) methods like peak-picking [18,19] or circle-fit approach [20,21]. Despite that, some studies addressed multiple degree-of-freedom (MDOF) approaches [22–24] that overcome the limitations of SDOF methods [25]. These MDOF approaches were performed in simple plate-like elements, though, so only one direction was inspected corresponding to bending deformation.

Regarding single-camera 3D systems, preliminary studies on vibration and modal analysis have been performed. Single resonance vibration measurement were performed by Barone et al. [26] combining a mirror system with a low frame rate camera for larger cost reduction. Also, a simple vibration test was performed by Yu and Pan [27] to evaluate a methodology that employs a colour high speed camera with a beam splitter, colour filters and mirrors to obtain two perspectives from two colour channels. A deeper vibration analysis was also performed by Yu and Pan [28] consisting in a modal identification using the simple peak-picking method from a classical mirror-based system measurement. The FP + DIC technique has been also employed for modal and vibration analysis. A vibration-based damage assessment procedure was investigated by Felipe and Díaz [29]. Moreover, modal analysis using FP + DIC measurement was firstly explored using the SDOF circle-fit approach [30].

In this study, a more advanced modal analysis using the least-squares complex exponential method (LSCE) is originally performed on FP + DIC measurements. Actually, this is the first attempt to employ a MDOF approach with a single-camera 3D technique. Simultaneous measurement and analogous identification was performed using 3D-DIC to validate the results with a consolidated full-field technique. This is also the first comparison of the performance of these optical techniques for modal analysis. Unlike the previous studies, this work performs a 3D modal characterisation on large industrial curved panel, what implies greater practical interest than flat plate-like geometries. Moreover, the complex shape and modal behaviour of the panel made necessary to analyse every direction, what triplicates the available data, and allowed to explore the full-field 3D modal identification in both cases, eluded in the literature. Sensitivity of measurement was evaluated comparing measurement noise floor, which enabled to predict possible unsuccessful modal identification. Considering that both optical techniques had different points of view and direct pixel to pixel relation was not possible, mode shape correlation was assessed by means of Image Decomposition procedure through Chebyshev shape descriptors [31]. Results establish FP + DIC for cost-worthy modal characterisation according to its limitations.

2. Experimental setup

The experimental equipment and devices for FP + DIC and 3D-DIC were prepared for simultaneous and synchronous measurement. A schematic arrangement of the described setup is in Fig. 1, including a panoramic photography. As this study involves measuring through these two DIC-based techniques, a speckle pattern must be present in the specimen surface. Nevertheless, the use of FP for 3D measurement in combination with 2D-DIC requires an additional fringe pattern. Employing a red speckle and blue fringes as shown in Fig. 1(b), it was possible to filter each pattern out by means of a Bayesian filter. For this purpose, the panel was coated with white paint background and, subsequently, red dots were randomly painted using a marker pen to create the speckle. A speckle mean size of 6 pixels was ensured to obtain an adequate contrast. Superimposed, blue fringes were generated by an Epson W32 projector. A single colour high speed camera model SA3 (1 Mpixel) by Photron with a Vivitar lens (28 mm focal length) was devoted for FP + DIC measurement. The result was a pair of images individually containing speckle for 2D-DIC and fringes for FP. On the other hand, two black-and-white high speed cameras model Photron SA4 (1 Mpixel) performed stereoscopic vision for 3D-DIC provided with 50 mm focal length Nikkon lenses. The red speckle were also exploited by this technique for what was required to erase blue fringe pattern with colour filter in lenses.

The tested specimen is an industrial composite panel of 1.45 m high, 2.0 m wide and 0.6 m deep, roughly. Its non-flat shape is also accentuated by three horizontal stiffeners. During the test, the panel hanged from a frame structure to reproduce free-free vibration. A shaker model Data Physics GW-V20/PA30E was installed behind the panel to generate a centred pointwise excitation in the lower edge. During the test, a noise random signal from 10 to 125 Hz was applied as excitation. A load cell (model HBM CFT/20 kN) was installed to register the resulting force signal that excited the shaker. Force signal acquisition was carried out by a NI USB-6251 DAQ. This device was synchronised with the three cameras so that cameras and load cell recorded 250 samples per second. Despite the fact that the pronounced curvature of the panel provides a meaningful example to show the capabilities of such techniques for 3D characterisation, it complicated the visualisation of the whole surface. Hence, under a symmetry assumption, the left half of the panel was exclusively studied allowing for measurement on two almost perpendicular surfaces.

3. Image processing and modal analysis

As stated previously, the recording process was accurately synchronised. However, the image sequence length differs from one camera model to another due to the internal memory. Therefore, whereas black-and-white cameras were able to obtain 5457 images at full-resolution, colour camera captured 1361 images.

For FP + DIC processing, colour images (Fig. 2(a)) were decomposed into an image where the speckle pattern is observed (Fig. 2(b)) and another one for the fringe pattern (Fig. 2(c)). Speckle images were processed using a commercial 2D-DIC algorithm (VIC 2D from Correlated Solutions Inc.) employing 29 pixels per subset and a 1 pixel step size. Besides, fringe pattern images were processed using a Fourier Profilometry [5] combined with a quality guided unwrapping algorithm [32] to obtain a 3D-shape map. Calibration of FP + DIC system was performed according to established procedures [7,33]. For that purpose, a smaller panel (rigid flat panel of 1 × 1 m) was placed at 3.75 m from optical axis of the camera and at three different positions (left, centre and right) as performed in previous investigations [29]. The calibration parameters of this setup was defined by an optical magnification of 2.2 mm/pixel and a mean fringe pattern pitch of 8.7 pixels (on the reference plane), which leads to a fringe relation of 8.5 mm/radian and a minimum uncertainty was considered of 0.470 mm [29]. Since FP measures the Z displacement as a variation of phase of the sinusoidal projected fringe pattern, the fringe relation associate the

Please cite this article as: Á. J. Molina-Viedma, L. Felipe-Sesé, E. López-Alba et al., Comparative of conventional and alternative Digital Image Correlation techniques for 3D modal characterisation, Measurement, https://doi.org/10.1016/j.measurement.2019.107101

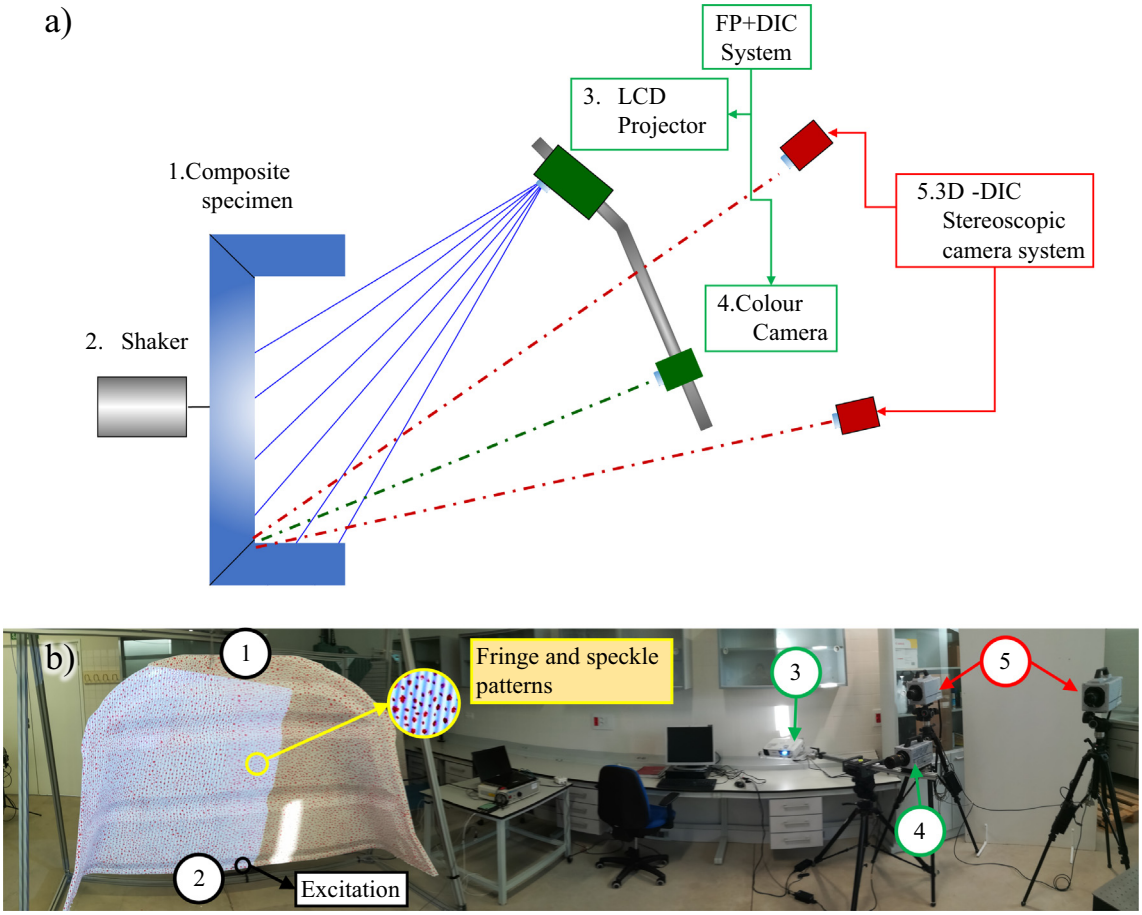

Fig. 1. (a) Schematic and (b) panoramic view of the experimental setup for FP + DIC and 3D-DIC vibration measurement on the composite panel (1) excited by a shaker (2). Highlighted in green is presented the FP + DIC system, consisted of the LCD projector (3) and the high speed colour camera (4). In red, the conventional 3D-DIC system composed of two black-and-white high speed cameras (5). (For interpretation of the references to colour in this figure legend, the reader is referred to the web version of this article.)

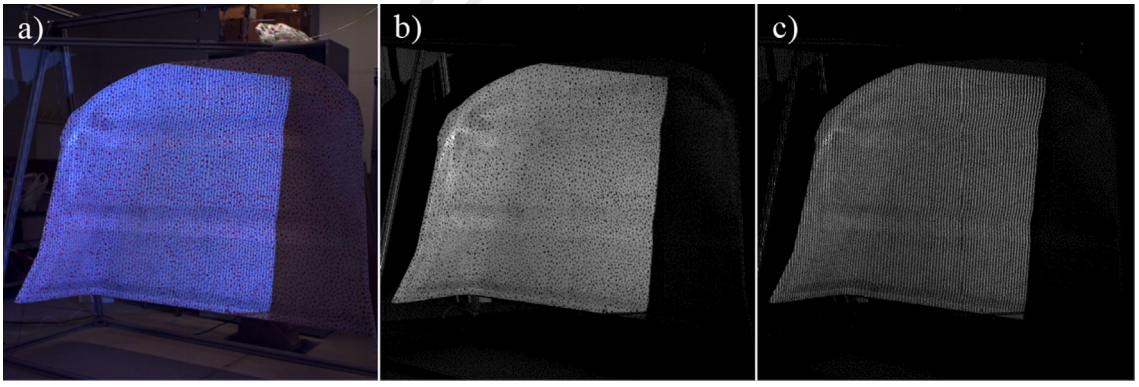

Fig. 2. Filtering of the (a) original image from the colour camera to obtain (b) speckle pattern and (c) fringe pattern.

phase measured by the FP procedure with the actual displacement experimented in the Z direction [7].

On the other hand, 3D-DIC required the analysis of the stereo camera system which were previously calibrated to determine the intrinsic and extrinsic parameters of the stereoscopic system. Then, DIC processing using VIC 3D software from Correlated Solutions Inc was performed using a 27 pixels facet size with a 4 pixel overlap step.

As a result, both techniques provided the time histories of X, Y and Z displacements corresponding to lateral, vertical and out-of plane directions from a very high spatial density mesh. Conventional FRF estimation was then performed for each measurement point. In order to obtain the same number of frequency lines, the window size was 750 points for each technique with 250 points overlap step to reduce the level of noise during windows averaging. As the number of images for FP + DIC obtained from one cap-

Please cite this article as: Á. J. Molina-Viedma, L. Felipe-Sesé, E. López-Alba et al., Comparative of conventional and alternative Digital Image Correlation techniques for 3D modal characterisation, Measurement, https://doi.org/10.1016/j.measurement.2019.107101

ture (1361 images) was relatively low regarding the window size, three complete captures were performed and the three resulting 3D-FRFs matrices were averaged. Modal identification was then performed using the LSCE method available in the Signal Processing MATLAB toolbox.

4. Results

4.1. PSDs comparative and noise floor evaluation

Despite the cost reduction of FP + DIC as a single camera 3D technique, this sort of technique could involve some issues related to image resolution (due to Bayer filtering and RGB encoding [9]) and hence uncertainty increasing. This has incidence on postprocessing results such as the modal parameters. Nevertheless, the quality of the measurements can be previously evaluated so that modal identification could be optimised in any case. Here, frequency domain signals are inspected for this purpose. Averaged auto-power spectral densities of two points of the panel measured with 3D-DIC and FP + DIC are shown in Fig. 3. As can be observed, both techniques yields similar results in high response frequency bands. However, higher 3D-DIC sensitivity is revealed in low response areas, being more pronounced as frequency increases. In this cases, FP + DIC reaches the noise floor and is unable to detect response peaks that are mostly clear for 3D-DIC. Despite reaching this level, detected high response peaks have major weight on modal identification. Therefore, FP + DIC modal identification was truncated to 100 Hz from where the response was mostly overcome by the noise floor, as seen in the plots.

4.2. Modal identification

In this work, the FRF matrix of each technique is composed of the three FRFs for X, Y and Z displacements of every single measurement point. The stabilisation diagram of each matrix is shown in Fig. 4. In both cases, the spectrum below 10 Hz was omitted since no excitation was applied there and, particularly, the upper limit of the spectrum was 100 Hz for FP + DIC, as explained above. In both cases, the LSCE method was able to identify clearly stable modes for both prominent and subtle peaks. The chosen model order for 3D-DIC was 22, where all the analysed modes were stable. During the modal identification, the computational modes where omitted according to incongruent damping values and mode shapes. As a result, ten modes were obtained. Analogously, the model order 23 was employed for FP + DIC.

Natural frequencies and structural damping ratios of those modes are shown in Table 1. As 3D displacements were assessed, 3D mode shapes were hence obtained. An example is shown in Fig. 5 corresponding to the third mode. However, to avoid the multiplicity of figures, the magnitude was used to represent the mode shapes of the seven common modes, as presented in Fig. 6. The numerical comparison of these maps entails some difficulties regarding the orientation and position of the mesh of each technique. To overcome this, mode shapes were decomposed into shape descriptors using Chebyshev polynomials according to concordance criteria [34]. This decomposition is insensitive to translations and rotation of the reference system and the result is a feature vector that contains the coefficient of each polynomial for the decomposed mode [31,35,36]. In this case, 80 shape descriptors were enough to reconstruct mode shapes with higher correlation coefficient than 90%. Hence, the feature vectors from each technique were equivalent and the correlation coefficient between them could be calculated [37]. The result is also included in Table 1. Those modes that only 3D-DIC was able to identify are shown in Fig. 7 for three directions.

5. Discussions

As a result of employing the LSCE method, modal parameters have been obtained employing 3D full-field techniques. Previously,

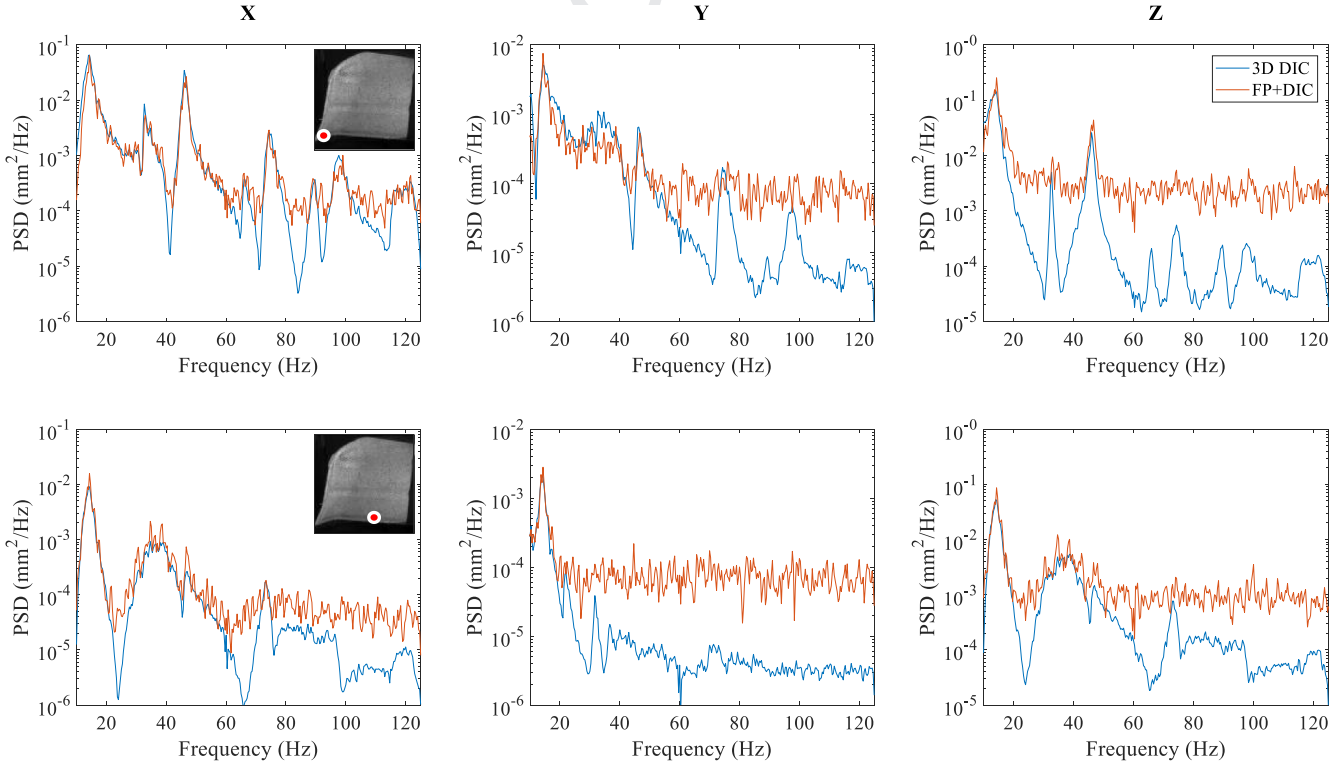

Fig. 3. Auto-PSDs of 3D displacements obtained with 3D-DIC and FP + DIC at a point in the left lower corner and close to the excitation point.

Please cite this article as: Á. J. Molina-Viedma, L. Felipe-Sesé, E. López-Alba et al., Comparative of conventional and alternative Digital Image Correlation techniques for 3D modal characterisation, Measurement, https://doi.org/10.1016/j.measurement.2019.107101

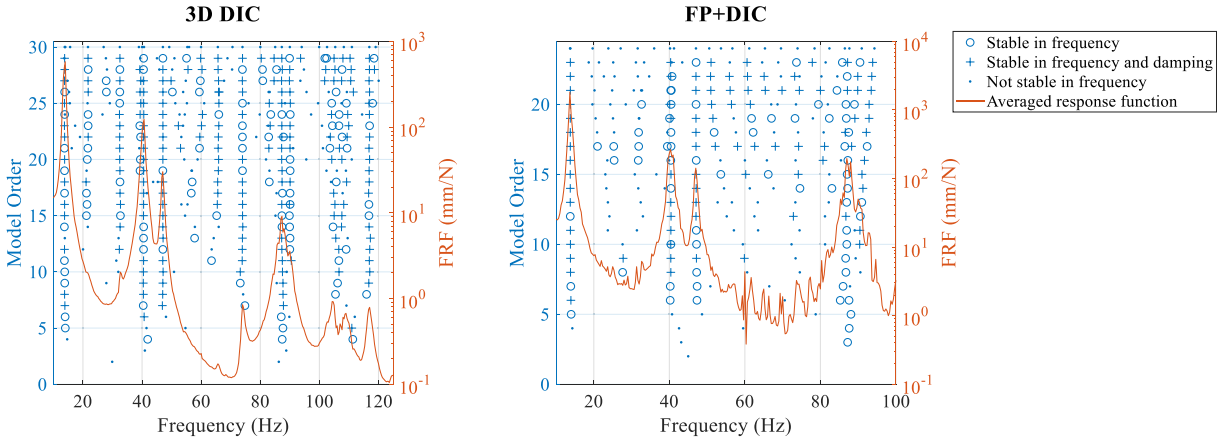

Fig. 4. Stabilisation diagrams obtained from 3D-DIC and FP + DIC measurements.

Table 1
Natural frequencies and structural damping ratios of the mode obtained with 3D-DIC and FP + DIC as well as the correlation coefficient of the shapes.

Mode	Frequency (Hz)		Structural damping (%)		Mode shape correlation
	3D-DIC	FP + DIC	3D-DIC	FP + DIC	
1	13.82	13.78	3.92	3.10	0.9575
2	32.43	31.97	2.58	13.94	0.9078
3	40.58	40.39	2.82	2.94	0.9675
4	47.04	47.08	1.88	2.02	0.9017
5	66.01	–	3.26	–	–
6	74.01	73.56	1.60	4.46	0.9294
7	87.45	87.29	2.86	2.14	0.8470
8	90.08	90.59	1.64	2.96	0.8548
9	104.42	–	2.74	–	–
10	116.98	–	1.72	–	–

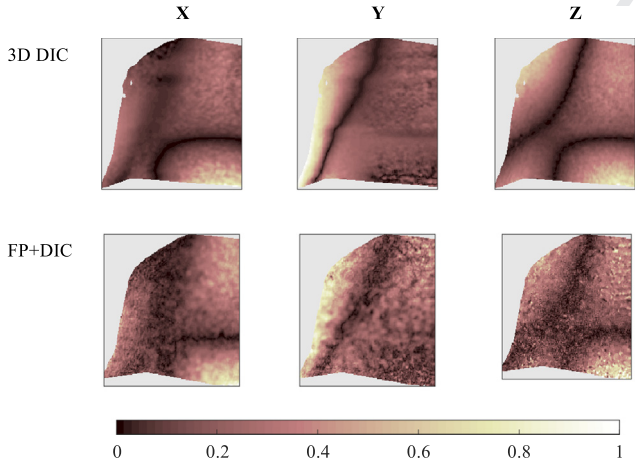

Fig. 5. Three-dimensional shape of the third mode (40 Hz) obtained with 3D-DIC and FP + DIC.

PSDs inspection revealed lower sensitivity of the single-camera FP + DIC system regarding conventional 3D-DIC. Observing the PSD in Z direction at the corner of the panel (Fig. 3), the noise floor for FP + DIC is about 3×10^{-3} mm^2/Hz, what in terms of displacement amplitude is 0.0447 mm, i.e., 0.007% of the specimen depth. In the same point of the panel, predominant peaks at 14 Hz and 47 Hz have a Z amplitude of 0.362 mm and 0.140 mm, respectively. Despite noise presence affects the resonances detection and stabilisation in FP + DIC measurement, with greater presence of computational modes, LSCE modal identification was able to identify seven identical modes for both techniques up to 90 Hz. For 3D-DIC, both its stabilisation diagram (Fig. 4) and its mode shapes (Fig. 6) have low presence of noise. For Z direction, the 3D-DIC noise floor is about 2.0×10^{-5} mm^2/Hz so the displacements amplitude is 0.0037 mm, i.e., one order inferior to FP + DIC. Therefore, it was able to describe peaks under the FP + DIC noise floor, highlighting amplitudes less than 5 μm for in-plane directions, X and Y. Therefore, modal parameter of FP + DIC were evaluated considering 3D-DIC as reference. Table 1 shows consistent natural frequencies. The identification of this parameter is typically less affected by the presence of noise, though. The highest response modes, as observed in the averaged FRF in the stabilisation diagram, are the first (14 Hz), the third (40 Hz) and the fourth (47 Hz). For such modes, structural damping estimation from FP + DIC is very similar to 3D-DIC. Moreover, mode shapes are clearly discernible and equivalent to 3D-DIC ones. That is quantitatively supported by high correlation coefficients. Among the remaining modes, the second one is especially remarkable since lower order modes are more easily detected by optical techniques due to the higher displacements. Conversely, the response of this mode is quite low and hence modal identification loses accuracy for FP + DIC. The mode shape is very noisy and the damping is not just dissimilar but also out of range for low-damped structures. This mode beside the sixth show the highest divergence regarding structural damping. In both cases, the reason for low response is that excitation was applied in a zero-displacement node as can be deduced from the 3D-DIC mode shapes. The symmetry of the panel make it probable that nodes appear in the symmetry edge of the panel, where it was excited. The same occurs for the fifth mode, shown in Fig. 7, which was not even detected by FP + DIC properly to be consider. For seventh and eighth modes, the excitation point was not a node as observed in 3D-DIC shapes. Therefore, the high level of noise in the mode shapes is just due to displace-

Please cite this article as: Á. J. Molina-Viedma, L. Felipe-Sesé, E. López-Alba et al., Comparative of conventional and alternative Digital Image Correlation techniques for 3D modal characterisation, Measurement, https://doi.org/10.1016/j.measurement.2019.107101

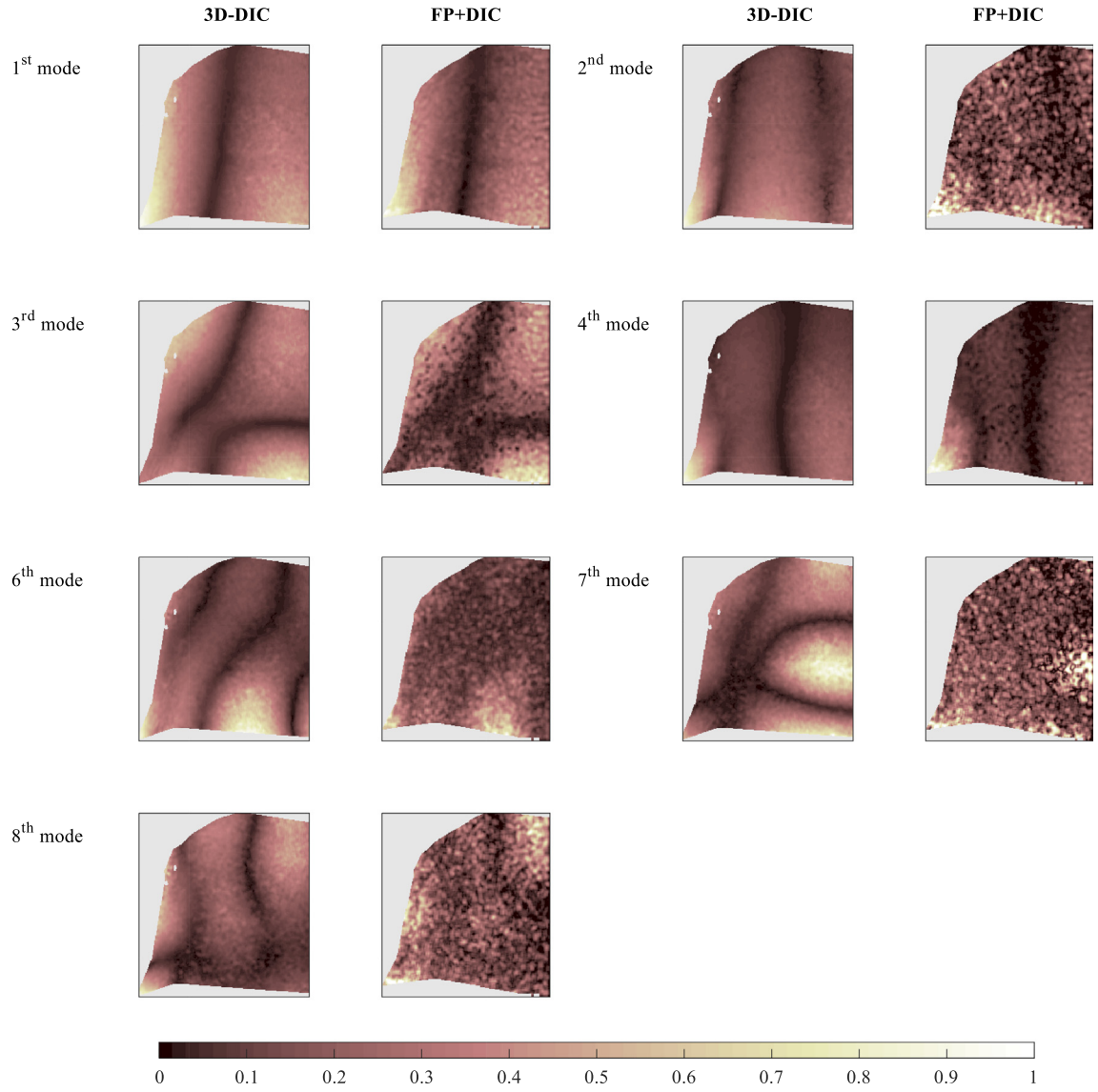

Fig. 6. Mode shape magnitude of the modes obtained by both 3D-DIC and FP + DIC.

ment amplitude reduction as frequency increases. Indeed, it was introduced in the PSDs inspection that response was mostly under noise floor for these frequencies except the highest response regions of each shape. Despite that, modal information is still retained [38] and modes shapes show an appreciable trend that is confirmed by correlation coefficient about 85%. It is important to highlight that out of plane sensitivity could be increased as the angle of the projector increases (which entails more distance between camera and projector) or smaller period of the grid. In this study, the former was not possible due to setup restrictions; higher distance would affect the stability of the optical assembly and hence the calibration. Additionally, smaller grid period would require higher camera resolution.

For modes exclusively assessed by 3D-DIC, the higher capacities of this technique are demonstrated. Fig. 7 still presents impressive mode shapes even when these modes provides very low response under this configuration. Actually, these results demonstrate that the capabilities of this technique could go beyond the frequency range here analysed.

6. Conclusions

This study has comparatively evaluated for the first time the capabilities of two DIC-based techniques such as FP + DIC and 3D-DIC itself for 3D modal characterisation using a MDOF approach. In terms of hardware, FP + DIC entails cost reduction by replacing one of the cameras by a standard projector. The study has been performed under equivalent conditions and measurements were performed on a complex aeronautical panel what makes it more representative of industrial applications than the typical flat plate structures. Additionally, the whole 3D information was exploited due to the curved panel shape. As an important novelty, this first comparison with 3D-DIC for modal analyses yielded a successful 3D modal analysis, including complicated mode shapes.

However this study has also evidenced that the economic and computational simplicity implications of removing a camera involves on the other hand some issues. The employed setup was restricted by the distances between the camera and the projector

Please cite this article as: Á. J. Molina-Viedma, L. Felipe-Sesé, E. López-Alba et al., Comparative of conventional and alternative Digital Image Correlation techniques for 3D modal characterisation, Measurement, https://doi.org/10.1016/j.measurement.2019.107101

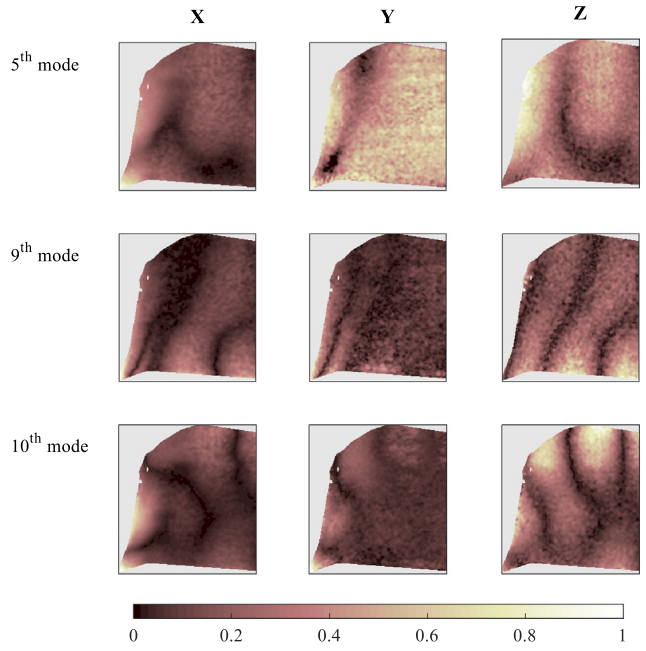

Fig. 7. Three-dimensional shape of the modes exclusively obtained with 3D-DIC.

which leaded to lower sensitivity of FP + DIC compared with 3D-DIC as observed in the measurement noise floor level. Modal identification was hence affected in the case of certain modes, especially at higher frequencies. However, 3D-DIC demonstrated to be able to characterise every mode in this spectrum. In fact, the quality of the results suggests 3D-DIC would have been able to explore higher spectrum in the present case. Despite the limitations, it has been proved that FP + DIC is able to provide a good performance for low frequency modal characterisation even for large elements and structures. Thus, FP + DIC entails a balance between budget and performance for experimental modal analysis, what may be significantly beneficial for flexible structures.

Declaration of Competing Interest

The authors declare that they have no known competing financial interests or personal relationships that could have appeared to influence the work reported in this paper.

References

[1] H. Schreier, J.-J. Orteu, M.A. Sutton, in: Image Correlation for Shape, Motion and Deformation Measurements, Springer US, Boston, MA, MA, 2009, https://doi.org/10.1007/978-0-387-78747-3.
[2] B. Pan, Digital image correlation for surface deformation measurement: historical developments, recent advances and future goals, Meas. Sci. Technol. 29 (2018), https://doi.org/10.1088/1361-6501/aac55b.
[3] B. Pan, L. Yu, Q. Zhang, Review of single-camera stereo-digital image correlation techniques for full-field 3D shape and deformation measurement, Sci. China Technol. Sci. 61 (2018) 2–20, https://doi.org/10.1007/s11431-017-9090-x.
[4] E. López-Alba, L. Felipe-Sesé, S. Schmeer, F.A. Díaz, Optical low-cost and portable arrangement for full field 3D displacement measurement using a single camera, Meas. Sci. Technol. 27 (2016), https://doi.org/10.1088/0957-0233/27/11/115901 115901.
[5] M. Takeda, K. Mutoh, Fourier transform profilometry for the automatic measurement of 3-D object shapes, Appl. Opt. 22 (1983) 3977, https://doi.org/10.1364/AO.22.003977.
[6] L. Felipe-Sesé, P. Siegmann, F.A. Díaz, E.A. Patterson, Simultaneous in-and-out-of-plane displacement measurements using fringe projection and digital image correlation, Opt. Lasers Eng. 52 (2014) 66–74, https://doi.org/10.1016/j.optlaseng.2013.07.025.
[7] L. Felipe-Sesé, P. Siegmann, F.A. Díaz, E.A. Patterson, Integrating fringe projection and digital image correlation for high-quality measurements of shape changes, Opt. Eng. 53 (2014), https://doi.org/10.1117/1.OE.53.4.044106 044106.
[8] P. Siegmann, V. Álvarez-Fernández, F. Díaz-Garrido, E.A. Patterson, A simultaneous in- and out-of-plane displacement measurement method, Opt. Lett. 36 (2011) 10, https://doi.org/10.1364/OL.36.000010.
[9] L. Felipe-Sesé, Á.J. Molina-Viedma, E. López-Alba, F.A. Díaz, RGB colour encoding improvement for three-dimensional shapes and displacement measurement using the integration of fringe projection and digital image correlation, Sensors (Switzerland) 18 (2018), https://doi.org/10.3390/s18093130.
[10] J. Baqersad, P. Poozesh, C. Niezrecki, P. Avitabile, Photogrammetry and optical methods in structural dynamics – a review, Mech. Syst. Signal Process. 86 (2017) 17–34, https://doi.org/10.1016/j.ymssp.2016.02.011.
[11] M.N. Helfrick, C. Niezrecki, P. Avitabile, T. Schmidt, 3D digital image correlation methods for full-field vibration measurement, Mech. Syst. Signal Process. 25 (2011) 917–927, https://doi.org/10.1016/j.ymssp.2010.08.013.
[12] N.S. Ha, T. Jin, N.S. Goo, Modal analysis of an artificial wing mimicking an Allomyrina dichotoma beetle's hind wing for flapping-wing micro air vehicles by noncontact measurement techniques, Opt. Lasers Eng. 51 (2013) 560–570, https://doi.org/10.1016/j.optlaseng.2012.12.012.
[13] D.A. Ehrhardt, M.S. Allen, S. Yang, T.J. Beberniss, Full-field linear and nonlinear measurements using Continuous-Scan Laser Doppler Vibrometry and high speed Three-Dimensional Digital Image Correlation, Mech. Syst. Signal Process. 86 (2017) 82–97, https://doi.org/10.1016/j.ymssp.2015.12.003.
[14] A.J. Molina-Viedma, L. Felipe-Sesé, E. López-Alba, F. Díaz, High frequency mode shapes characterisation using Digital Image Correlation and phase-based motion magnification, Mech. Syst. Signal Process. 102 (2018) 245–261, https://doi.org/10.1016/j.ymssp.2017.09.019.
[15] A.J. Molina-Viedma, L. Felipe-Sesé, E. López-Alba, F.A. Díaz, 3D mode shapes characterisation using phase-based motion magnification in large structures using stereoscopic DIC, Mech. Syst. Signal Process. 108 (2018) 140–155, https://doi.org/10.1016/j.ymssp.2018.02.006.
[16] Á. Molina-Viedma, E. López-Alba, L. Felipe-Sesé, F. Díaz, J. Rodríguez-Ahlquist, M. Iglesias-Vallejo, Modal parameters evaluation in a full-scale aircraft demonstrator under different environmental conditions using HS 3D-DIC, Materials (Basel) 11 (2018) 230, https://doi.org/10.3390/ma11020230.
[17] C. Warren, C. Niezrecki, P. Avitabile, P. Pingle, Comparison of FRF measurements and mode shapes determined using optically image based, laser, and accelerometer measurements, Mech. Syst. Signal Process. 25 (2011) 2191–2202, https://doi.org/10.1016/j.ymssp.2011.01.018.
[18] F. Trebuňa, M. Hagara, Experimental modal analysis performed by high-speed digital image correlation system, Measurement 50 (2014) 78–85, https://doi.org/10.1016/j.measurement.2013.12.038.
[19] N.S. Ha, H.M. Vang, N.S. Goo, Modal analysis using digital image correlation technique: an application to artificial wing mimicking beetle's hind wing, Exp. Mech. (2015) 989–998, https://doi.org/10.1007/s11340-015-9987-2.
[20] Á.J. Molina-Viedma, E. López-Alba, L. Felipe-Sesé, F.A. Díaz, Full-field modal analysis during base motion excitation using high-speed 3D digital image correlation, Meas. Sci. Technol. 28 (2017), https://doi.org/10.1088/1361-6501/aa7d87 105402.
[21] Á. Molina-Viedma, E. López-Alba, L. Felipe-Sesé, F. Díaz, Modal identification in an automotive multi-component system using HS 3D-DIC, Materials (Basel) 11 (2018) 241, https://doi.org/10.3390/ma11020241.
[22] W. Wang, J.E. Mottershead, T. Siebert, A. Pipino, Frequency response functions of shape features from full-field vibration measurements using digital image correlation, Mech. Syst. Signal Process. 28 (2012) 333–347, https://doi.org/10.1016/j.ymssp.2011.11.023.
[23] R. Huňady, M. Hagara, A new procedure of modal parameter estimation for high-speed digital image correlation, Mech. Syst. Signal Process. 93 (2017) 66–79, https://doi.org/10.1016/j.ymssp.2017.02.010.
[24] P.L. Reu, D.P. Rohe, L.D. Jacobs, Comparison of DIC and LDV for practical vibration and modal measurements, Mech. Syst. Signal Process. 86 (2017) 2–16, https://doi.org/10.1016/j.ymssp.2016.02.006.
[25] D.J. Ewins, Modal Testing: Theory, Practice, and Application, second ed., Research Studies Press LTD, Baldock, Hertfordshire, England, 2000.
[26] S. Barone, P. Neri, A. Paoli, A.V. Razionale, Low-frame-rate single camera system for 3D full-field high-frequency vibration measurements, Mech. Syst. Signal Process. 123 (2019) 143–152, https://doi.org/10.1016/j.ymssp.2019.01.016.
[27] L. Yu, B. Pan, Full-frame, high-speed 3D shape and deformation measurements using stereo-digital image correlation and a single color high-speed camera, Opt. Lasers Eng. 95 (2017) 17–25, https://doi.org/10.1016/j.optlaseng.2017.03.009.
[28] L. Yu, B. Pan, Single-camera high-speed stereo-digital image correlation for full-field vibration measurement, Mech. Syst. Signal Process. 94 (2017) 374–383, https://doi.org/10.1016/j.ymssp.2017.03.008.
[29] L. Felipe-Sesé, F.A. Díaz, Damage methodology approach on a composite panel based on a combination of Fringe Projection and 2D Digital Image Correlation, Mech. Syst. Signal Process. 101 (2018) 467–479, https://doi.org/10.1016/j.ymssp.2017.09.002.
[30] L. Felipe-Sesé, Á.J. Molina-Viedma, E. López-Alba, F.A. Díaz, FP+DIC for low-cost 3D full-field experimental modal analysis in industrial components, Mech. Syst. Signal Process. 128 (2019) 329–339, https://doi.org/10.1016/j.ymssp.2019.04.004.
[31] C. Sebastian, E. Hack, E. Patterson, An approach to the validation of computational solid mechanics models for strain analysis, J. Strain Anal. Eng. Des. 48 (2013) 36–47, https://doi.org/10.1177/0309324712453409.

Please cite this article as: Á. J. Molina-Viedma, L. Felipe-Sesé, E. López-Alba et al., Comparative of conventional and alternative Digital Image Correlation techniques for 3D modal characterisation, Measurement, https://doi.org/10.1016/j.measurement.2019.107101

[32] D. Ghiglia, M. Pritt, Two-dimensional phase unwrapping: theory, algorithms, and software, 1998. doi:10.1177/004057368303900411.
[33] P. Siegmann, L. Felipe-Sese, F. Diaz-Garrido, Improved 3D displacement measurements method and calibration of a combined fringe projection and 2D-DIC system, Opt. Lasers Eng. 88 (2017) 255–264, https://doi.org/10.1016/j.optlaseng.2016.08.014.
[34] R.L. Burguete, G. Lampeas, J.E. Mottershead, E.A. Patterson, A. Pipino, T. Siebert, W. Wang, Analysis of displacement fields from a high-speed impact using shape descriptors, J. Strain Anal. Eng. Des. 49 (2014) 212–223, https://doi.org/10.1177/0309324713498074.
[35] E. Lopez-Alba, C.M. Sebastian, W.J. Christian, E.A. Patterson, The use of charge-coupled device cameras for characterizing the mean deflected shape of an aerospace panel during broadband excitation, J. Strain Anal. Eng. Des. (2018), https://doi.org/10.1177/0309324718812542, 030932471881254.
[36] E. Lopez-Alba, C.M. Sebastian, A.C. Santos Silva, E.A. Patterson, Experimental study of mode shifting in an asymmetrically heated rectangular plate, J. Sound Vib. 439 (2019) 241–250, https://doi.org/10.1016/j.jsv.2018.09.044.
[37] L. Felipe-Sesé, F.A. Diaz-Garrido, E.A. Patterson, Exploiting measurement-based validation for a high-fidelity model of dynamic indentation of a hyperelastic material, Int. J. Solids Struct. 97–98 (2016) 520–529, https://doi.org/10.1016/j.ijsolstr.2016.06.036.
[38] J. Javh, J. Slavič, M. Boltežar, High frequency modal identification on noisy high-speed camera data, Mech. Syst. Signal Process. 98 (2018) 344–351, https://doi.org/10.1016/j.ymssp.2017.05.008.

Please cite this article as: Á. J. Molina-Viedma, L. Felipe-Sesé, E. López-Alba et al., Comparative of conventional and alternative Digital Image Correlation techniques for 3D modal characterisation, Measurement, https://doi.org/10.1016/j.measurement.2019.107101